

# Supporting Information

## **The sequestration mechanism as a generalizable approach to improve the sensitivity of biosensors and bioassays**

Alejandro Chamorro-Garcia<sup>1,2</sup>, Claudio Parolo<sup>3</sup>, Gabriel Ortega<sup>4,5</sup>, Andrea Idili<sup>2</sup>, Joshua Green<sup>6</sup>, Francesco Ricci<sup>2</sup> and Kevin W. Plaxco<sup>\*,1</sup>

---

<sup>1</sup> Department of Chemistry and Biochemistry University of California Santa Barbara (UCSB), Santa Barbara, CA 93106, USA.

<sup>2</sup> Dipartimento di Scienze e Tecnologie Chimiche, University of Rome, Tor Vergata, Via della Ricerca Scientifica, 00133 Rome, Italy

<sup>3</sup> ISGlobal - Barcelona Institute for Global Health, Carrer del Rosselló 132, 08036 Barcelona, Spain

<sup>4</sup> Ikerbasque, Basque Foundation for Science, 48013 Bilbao, Spain.

<sup>5</sup> Precision Medicine and Metabolism Laboratory, CIC bioGUNE, Basque Research and Technology Alliance, Parque Tecnológico de Bizkaia, Derio, Spain

\* Corresponding author: [kwp@ucsb.edu](mailto:kwp@ucsb.edu)

### **Target production (Neutrophil gelatinase-associated lipocalin, NGAL)**

We produced our target, the protein NGAL, following previously described protocols(1). Briefly, we used an ampicillin-resistance-encoding pET-21a plasmid containing the gene encoding for NGAL cloned between the restriction sites Nde I and Xho I (the plasmid was kindly provided by Aptitude, Inc., Santa Barbara, CA). The protein incorporates a hexa-histidine tag at its carboxy-terminus and cysteine to serine mutation at position 85, to facilitate protein expression and purification. The amino acid sequence of the resulting gene is:

```
MTSDLIPAPP LSKVPLQQNF QDNQFQGWY VVGLAGNAIL REDKDPQKMY  
ATYIELKEDK SYNVTSVLFR KKKCDYWIRT FVPGSQPGEF TLGNIKSYPG  
LTSYLVRVVS TNYNQHAMVF FKKVSNREY FKITLYGR TK ELTSELKENF  
IRFSKSLGLP ENHIVFPVPI DQCIDGLE HHHHHH
```

To obtain the protein we transformed the plasmid into *E. coli* BL21(DE3) cells (New England Biolabs, Ipswich, MA), and then induced expression using 1 mM IPTG for 4 h at 37°C. We lysed cells by ultrasound treatment and then performed His-tag affinity chromatography (HisTrap HP-5mL, GE Healthcare, Chicago, IL) and size exclusion chromatography (Superdex S100, GE Healthcare, Chicago, IL) in buffer 50 mM sodium phosphate (pH 7.0) and 100 mM sodium chloride. We then used spectrophotometry to assess protein concentration (molar absorption coefficient at 280 nm = 26,025 M<sup>-1</sup> cm<sup>-1</sup>). Typical yield was of order 50 mg/L of culture.

### **Aptamer affinity evaluation though ELISA**

In order to determine the affinities of the full-length and truncated (26-base) aptamers we performed enzyme-linked immunosorbent assays (ELISAs) in which we titrated biotinylated aptamer into NGAL-coated wells in a multi-well plate. We used HRP streptavidin conjugated as reporter to quantify the presence of aptamer in each well. In this, the wells were coated with NGAL at 100 nM in PBS, 50 µL per well, and incubated overnight at 4°C. The next day plates were washed using 100 µL of 0.05% (v/v) Tween 20 pH 7.4 PBS 3 times. Blocking was performed by adding 100 µL per well of 2% (w/v) BSA 0.05% (v/v) Tween 20 pH 7.4 PBS and incubating for 2 h

at room temperature in a thermoshaker. The wells were then washed 3 times with 100  $\mu\text{L}$  per well of 0.05% (v/v) Tween 20 pH 7.4 PBS. Next, 50  $\mu\text{L}$  of biotinylated aptamer at different concentrations in pH 7.4 PBS were added to the corresponding wells followed by incubation for 1 h at room temperature in a thermoshaker rotating at 650 rpm. The wells were the washed 3 times as described above and 50  $\mu\text{L}$  per well of streptavidin-HRP diluted to 100 ng/mL in 1% BSA 0.05% Tween 20 PBS pH 7.4 PBS buffer was added. We then incubated the plates for 30 min at room temperature and 650 rpm in a thermoshaker. The wells were the washed 3 times (above protocol), plus a additional wash using just pH 7.4 PBS. We the added 50  $\mu\text{L}$  per well of TMB reagent. After 2 min the reaction was stopped by adding 25  $\mu\text{L}$  per well of a 0.25 M  $\text{H}_2\text{SO}_4$  and after 15 min absorbance of each well was read at 450 nm. Error bars were calculated using the standard deviation of 4 repetitions of each point.

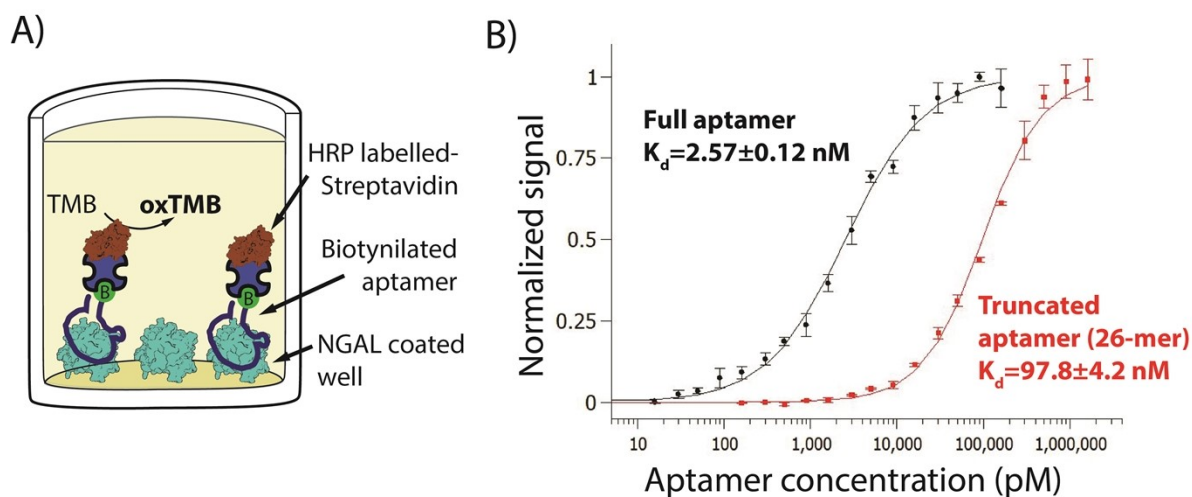


**Figure S11:** Using an ELISA assay (A) we demonstrate here the differing affinities of the full-length and truncated NGAL aptamers. The affinity of the full-length aptamer is almost 40 times greater than that of the truncated aptamer.

## Data analysis

We fit the binding curves of the different sensors and assays to the Hill equation:

$$Occupancy (\Theta) = \frac{[T]^{n_H}}{K_{1/2}^{n_H} + [T]^{n_H}} \quad (\text{Equation S1})$$

Where  $[T]$  is the concentration of NGAL,  $K_{1/2}$  the midpoint in the binding curve, and  $n_H$  the pseudo-Hill coefficient.

## Sequestration; theoretical model

The sequestration mechanism has previously been modelled by Buchler and co-workers(2) by applying the principle of mass balance to Equation 1:

$$[T]_t = [T] + [T - dep] \quad (\text{Equation S2})$$

$$[dep]_t = [dep] + [T - dep] \quad (\text{Equation S3})$$

Here  $[T]_t$  is the total target concentration,  $[T]$  is the free target concentration,  $[T-dep]$  is the concentration of target that is bound to the depletant,  $[dep]_t$  is the total depletant concentration, and  $[dep]$  the concentration of free depletant. Taking into account the equilibrium described by:

$$K_d^{dep} = \frac{[T] \cdot [dep]}{[T - dep]} \quad (\text{Equation S4})$$

where  $K_d^{dep}$  is the dissociation constant and  $[T-dep]$  the concentration of target bound to the depletant. When combining Equation 2 and 3 into Equation 4, we obtain an expression describing the concentration of free target:

$$[T] = \frac{1}{2} \left( [T]_t - [dep] - K_d^{dep} + \sqrt{([T]_t - [dep] - K_d^{dep})^2 + 4[T]_t K_d^{dep}} \right) \quad (\text{Equation S5})$$

Substituting equation 5 into equation 1 we obtain the Hill expression:

*Normalized  
Signal*

$$= \frac{\left[ \frac{1}{2} \left( [T]_t - [dep] - K_d^{dep} + \sqrt{([T]_t - [dep] - K_d^{dep})^2 + 4[T]_t K_d^{dep}} \right) \right]^{n_H}}{\left[ \frac{1}{2} \left( [T]_t - [dep] - K_d^{dep} + \sqrt{([T]_t - [dep] - K_d^{dep})^2 + 4[T]_t K_d^{dep}} \right) \right]^{n_H} + K_{1/2}^{n_H}}$$

(Equation S6)

Here  $n_H$  the intrinsic hill coefficient of the receptor (system in absence of depletant), and  $K_{1/2}$  the apparent dissociation constant of the receptor (in absence of depletant). The resulting expression, equation 6, is the one we used to model the theoretical sequestration response depicted in Figure 1 in the main text.

### Characterization of gold nanoparticles

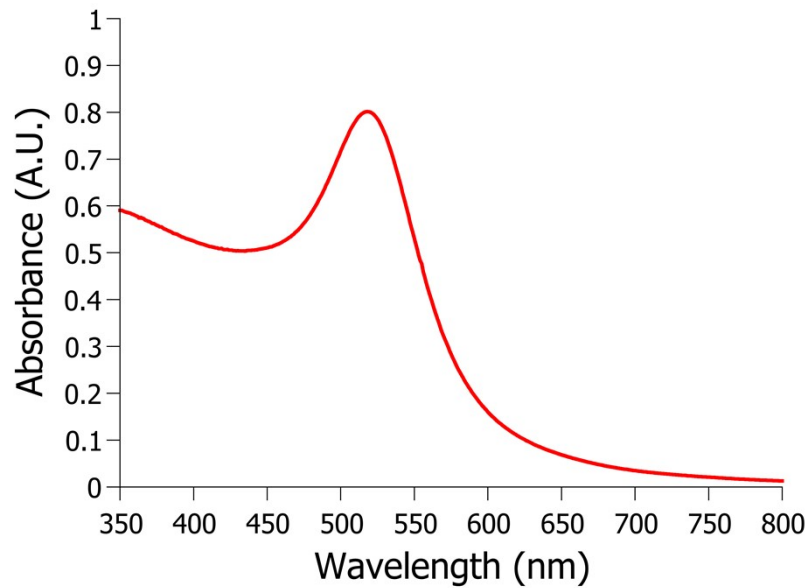


**Figure S12:** We characterized the gold nanoparticles synthesized for the dipstick assays by measuring their absorption spectra in water. The sharp absorbance peak centered at  $\sim 520$  nm confirms the proper reduction of gold into spherical structures of diameters  $\sim 20$  nm [refs(3, 4)].

### Dipstick assays

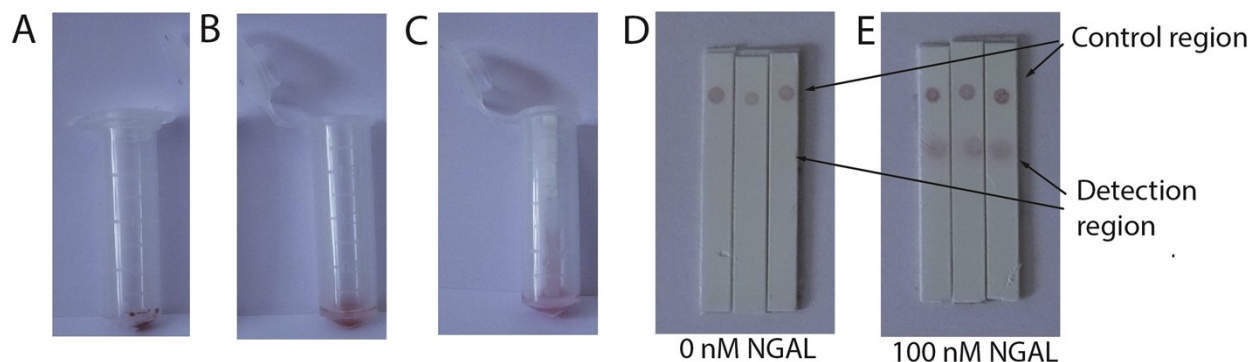


**Figure S13:** For the dipstick assays we lyophilized the gold-nanoparticle-modified antibodies in Eppendorf tubes (A). We then resuspended these in  $60\ \mu\text{L}$  of sample (B) before inserting the nitrocellulose strip to perform the dipstick assay. Once we added the strip to the tube the mixture of sample and gold-nanoparticle-conjugated antibodies flowed by capillarity through the strip (C). Once the assay concluded we trimmed the absorbent pads from the strips and scanned them to quantify their optical signal. For example, panel D) shows control strips (no NGAL), and panel E shows the results of a sample of 100 nM NGAL with no depletant.

### Improved sensitivity

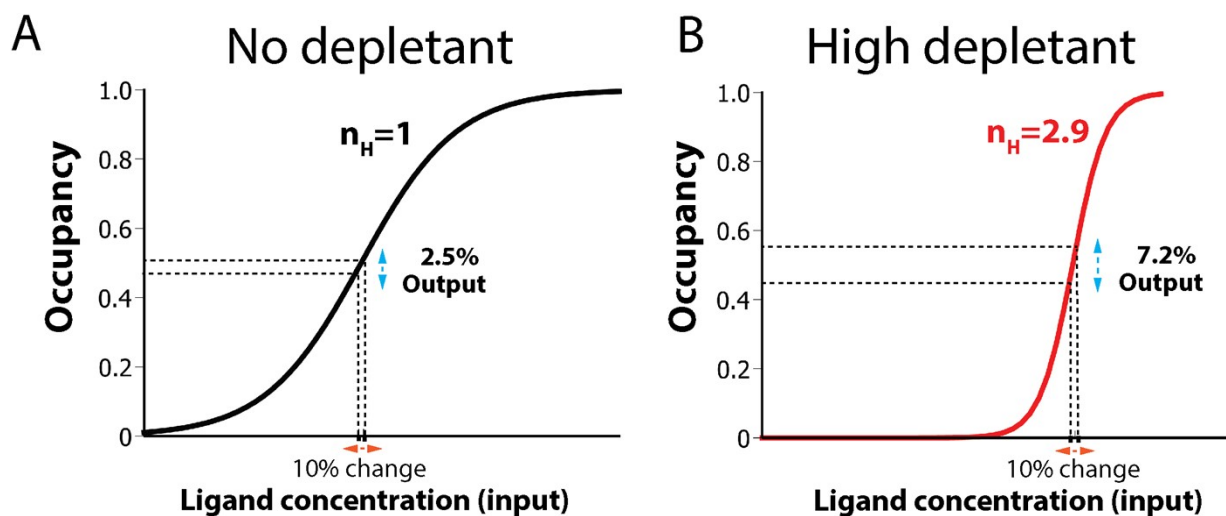


**Figure S14:** Steeper transitions result in more sensitive receptors. For example, for a receptor of  $n_H = 1$ , a change in target concentration from 5% below to 5% above the binding midpoint

changes occupancy –and the resulting output signal– by just 2.5%. In contrast, a receptor of  $n_H = 2.9$  produces a 7.2% change in output for the same change in input.

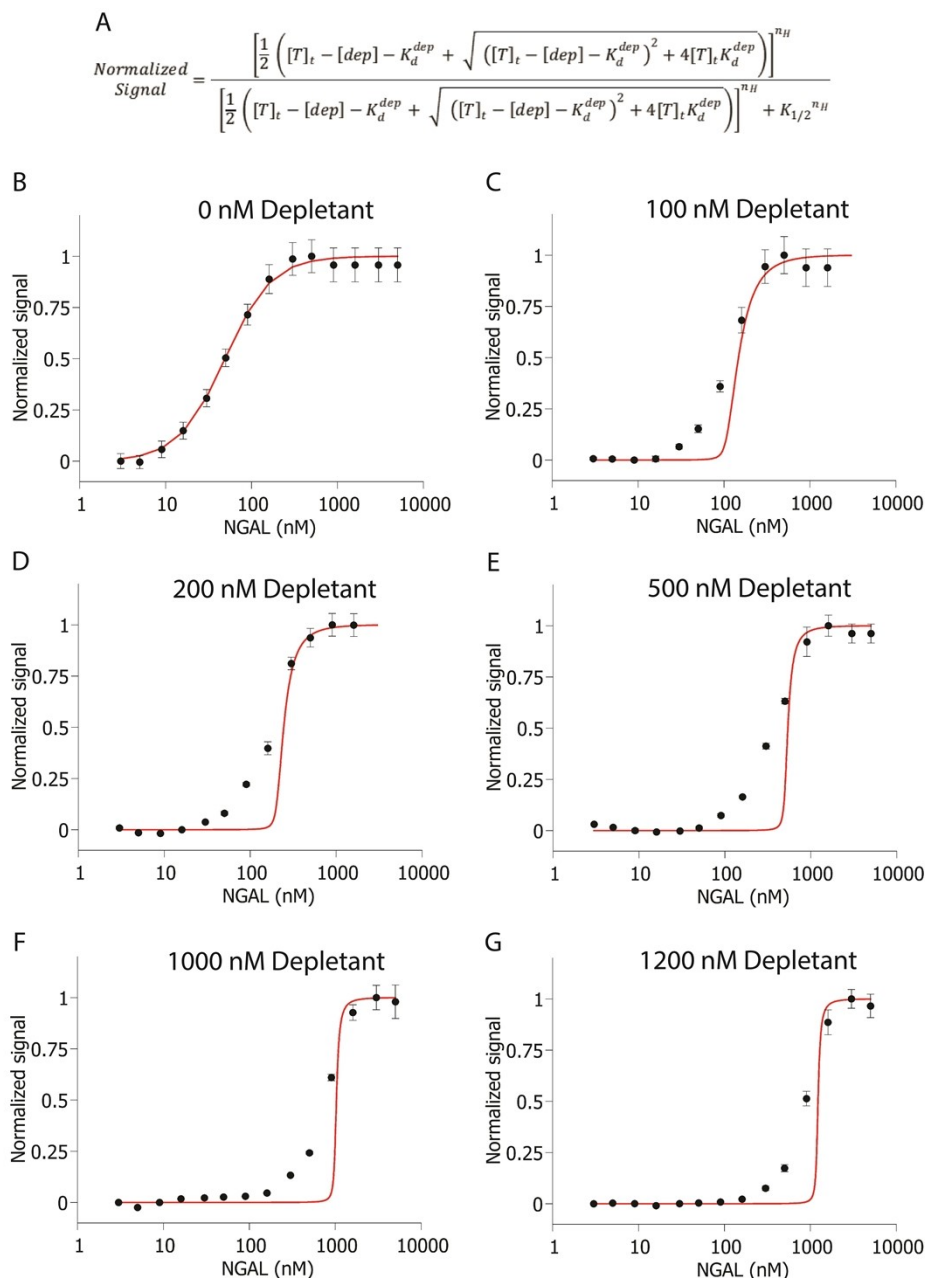


**Figure S15:** (A) Buchler Cross(2) have described the output expected for ideal sequestration. In this,  $[T]_t$  is total target concentration in the sample,  $[\text{dep}]$  is the concentration of depletant,  $K_d^{\text{dep}}$  is the dissociation constant of the depletant (in this model we used the reported affinity: 0.92 nM (5)),  $K_{1/2}$  is the apparent dissociation constant of the receptor in absence of depletant (for the EAB sensor 49 nM figure 2 in the main text), and  $n_H$  is the Hill coefficient of the receptor in absence of depletant (1.6 for the EAB sensor Figure 2 in the main text). (B-G) Experimental data (black dots) we collected from electrochemical aptamer-based (EAB) sensors fit to the Buchler model (red line) indicate that the improved sensitivity we observed is less than would be expected given this theory. We suspect that the resulting deviation are

likely arise due to both surface interactions complex matrix interactions, both of which can alter the ability of sequestration to steepen binding curves.

### References cited

1. C. Parolo, *et al.*, Real-Time Monitoring of a Protein Biomarker. *ACS Sensors* **5**, 1877–1881 (2020).
2. N. E. Buchler, F. R. Cross, Protein sequestration generates a flexible ultrasensitive response in a genetic network. *Mol. Syst. Biol.* **5**, 272 (2009).
3. J. Turkevich, P. C. Stevenson, J. Hillier, A study of the nucleation and growth processes in the synthesis of colloidal gold. *Discuss. Faraday Soc.* **11**, 55–75 (1951).
4. M.-C. Daniel, D. Astruc, Gold Nanoparticles: Assembly, Supramolecular Chemistry, Quantum-Size-Related Properties, and Applications toward Biology, Catalysis, and Nanotechnology. *Chem. Rev.* **104**, 293–346 (2004).
5. J. Wang, *et al.*, Multiparameter Particle Display (MPPD): A Quantitative Screening Method for the Discovery of Highly Specific Aptamers. *Angew. Chemie Int. Ed.* **56**, 744–747 (2017).